Available online at www.sciencedirect.com
ScienceDirect
Journal of Photochemistry and Photobiology A: Chemistry 196 (2008) 94–98
Journal of Photochemistry and Photobiology A:Chemistry
www.elsevier.com/locate/jphotochem

DNA detection via programmed core-shell nanodot-assembly with concomitant fluorescence modulation

Chang-Keun Lim [a], Hyun-Joong Kim [b], Hae-Yeong Kim [b], Youn Jung Kwon [c], Seung Won Paek [c], Soo Young Park [a,*]

[a] School of Materials Science and Engineering, Seoul National University, San 56-1 Shillim-dong, Kwanak-ku, Seoul 151-744, Republic of Korea
[b] Institute of Life Sciences & Resources and Graduate School of Biotechnology, Kyung Hee University, Suwon 449-701, Republic of Korea
[c] GeneChem Inc., 59-5 Jang-dong, Yuseong-gu, Daejeon 305-343, Republic of Korea

Received 6 September 2007; received in revised form 5 November 2007; accepted 20 November 2007
Available online 10 January 2008

Abstract

In this work, we designed and demonstrated a new DNA probe working on the principle of the fluorescence change with improved detection capability via building a cruciform DNA hybrid with target ODNs. In our oligodeoxynucleotide-pyrene-oligodeoxynucleotide (OPO) probe, hybridisations between the probes (OPO) and target oligodeoxynucleotides (ODNs) are programmed to induce the formation of core-shell (pyrene-ODN) nanodot structure in aqueous solution to generate and maintain their excimer emission more efficiently. Since this novel OPO probe showed wide detection range, high-excimer emission efficiency and high reliability of excimer emission intensity, the probe is capable of application to diagnosis of genetic disease and detection of increased DNA copy number and occurrence of mutation in a real-time PCR.

Keywords: DNA nanostructure; Excimer emission; Fluorescent probes; Real-time PCR; Nanobiotechnology

1. Introduction

Nucleic acids, with perfect binding capability, have been widely investigated not only for the diagnosis and therapy of various genetic diseases [1–3] but also for their use as building blocks and structure-directing components in so-called 'bottom-up' approach to generate self-assembled architectures with a precise control at the nanometer scale [4,5]. For the diagnostics of genetic disorders and infections of various etiologies, a number of hybridisation probes, which detect a specific sequence via optical, electrochemical or piezoelectric transduction, have been developed [6–9]. On the other hand, the highly specific self-assembly of oligonucleotides has been exploited to build one [10], two [11] and three [12] dimensional nanoarchitectures which have potential applications to chemistry, biology, electronics, computation and so on [13]. A creative approach combining both of these electronic/optical probing and self-assembling capabilities of hybridisation is believed to offer ever-broader spectrum of potential application in diagnostics and to extend the limits of nanobiotechnology.

Herein we designed a new DNA hybridisation probe working on the principle of the fluorescence change with improved detection capability via a condensed hybridisation to build a cruciform DNA hybrid with target ODNs. In our oligodeoxynucleotide-pyrene-oligodeoxynucleotide (OPO) probe, hybridisations between the probes (OPO) and target oligodeoxynucleotides (ODNs) are programmed to induce the formation of core-shell (pyrene-ODN) nanodot structure in aqueous solution to generate and maintain their excimer emission more efficiently (see Fig. 1).

2. Materials and methods

2.1. Instruments

NMR measurement was recorded on a Avance DPX-300 (300 MHz, Bruker) in DMSO-d_6 solution. Mass spectra were measured on a Voyager-DE^{TM} STR Biospectrometry Workstation (Applied Biosystems Inc.) by MALDI-ToF method. The data of elemental analysis was measured on EA1110 (CE

* Corresponding author. Tel.: +82 2 880 8032; fax: +82 2 886 8331.
E-mail address: parksy@snu.ac.kr (S.Y. Park).

1010-6030/$ – see front matter © 2008 Elsevier B.V. All rights reserved.
doi:10.1016/j.jphotochem.2007.11.019

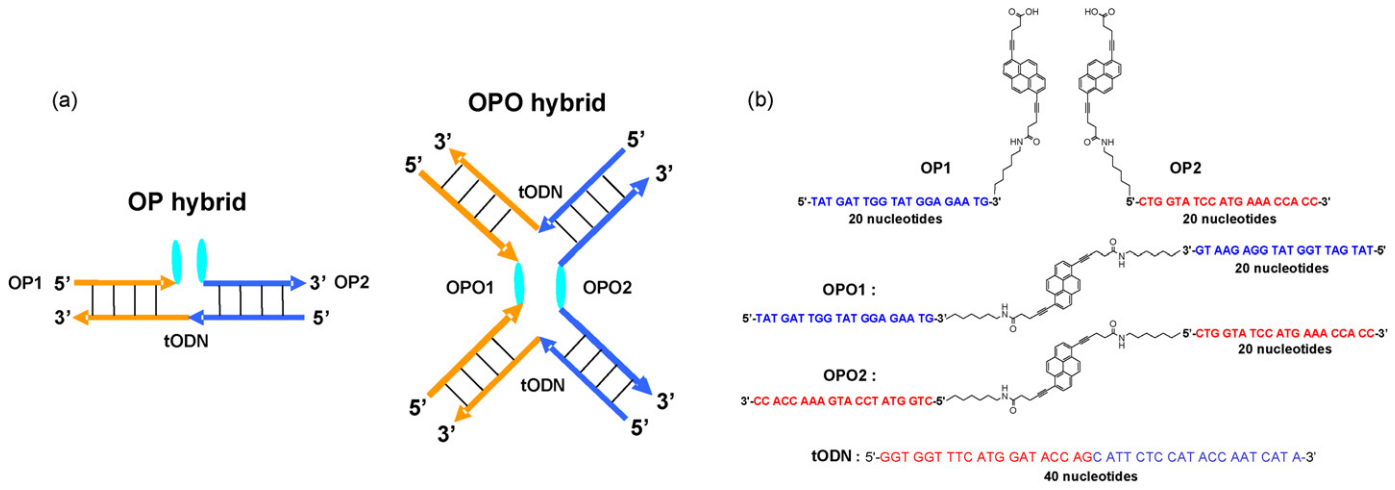

Fig. 1. Schematic representations of (a) hybridization of tODN and probes (OP and OPO) and (b) sequences of synthesized oligodeoxynucleotide derivatives.

Instrument). Fluorescence spectra were measured on a RF-500 spectrofluorophotometer (Shimadzu). ODNs were synthesized by EXPEDITE (Applied Biosystems Inc.) and purified on SCL-10A (Shimadzu) by HPLC. The HR-TEM images were obtained by JEM-4010 (JEOL).

2.2. Synthesis

2.2.1. Synthesis of bis(2,5-dioxopyrrolidin-1-yl)-5,5′-(pyrene-1,6-diyl)dipent-4-ynoate (NHS-Py-NHS)

Bis(2,5-dioxopyrrolidin-1-yl)-5,5′-(pyrene-1,6-diyl)dipent-4-ynoate (NHS-Py-NHS) was synthesized according to the literature method [14]. ^{1}H NMR (300 MHz, DMSO-d_6) δ (ppm): 8.52 (d, J = 9.1 Hz, 2H), 8.31 (d, J = 8.2 Hz, 2H), 8.28 (d, J = 9.1 Hz, 2H), 8.15 (d, J = 8.2 Hz, 2H), 3.21 (t, J = 6.2 Hz, 4H), 3.04 (t, J = 6.2 Hz, 4H), 2.87 (s, 8H). ^{13}C NMR (75 MHz, DMSO-d_6) δ [ppm]: 70.069, 167.849, 131.265, 130.330, 129.921, 128.223, 125.721, 125.277, 123.203, 118.029, 94.466, 79.766, 30.011, 25.444, 14.992. MS [M^+]: (MALDI-ToF (reflector mode)) calcd. for $C_{34}H_{24}N_2O_8$, 588.56; found, 588.35. Anal. calcd. for $C_{34}H_{24}N_2O_8$: C, 69.38; H, 4.11; N, 4.76. Found: C, 69.10; H, 4.29; N, 4.73.

2.2.2. Preparation of 5′-TAT GAT TGG TAT GGA GAA TG-3′-Py (OP1) and 5′-TAT GAT TGG TAT GGA GAA TG-3′-Py-3′-GT AAG AGG TAT GGT TAG ATA-5′ (OPO1)

HPLC purified 5′-TAT GAT TGG TAT GGA GAA TG-amine-3′ (39.6 O.D.) was dissolved in 100 μL 0.1 M sodium tetraborate–HCl buffer (pH 8.5) and 100 μL DMSO was added to the solution. NHS-Py-NHS dissolved in 100 μL DMSO was added to the solution and the mixture was shaken at r.t. for 12–18 h. The solution of 750 μL 100% cold ethanol and 30 μL 3 M sodium acetate (pH 5.2) was added to the mixture and stored at −70 °C for 40 min and then the mixture was centrifuged by 12,000 rpm at −4 °C for 20 min. The supernatant was removed and the precipitate was washed with 700 μL of 80% cold ethanol and then dried. The precipitate was purified with HPLC and the pure OP1 and OPO1 were obtained (30–40% yield). MS [M^+]: (MALDI-ToF (linear mode)) calcd. for OP1, 6792.67; found, 6788.8 and calcd. for OPO1, 13220.9; found, 13221.5.

2.2.3. Preparation of 3′-CC ACC AAA GTA CCT ATG GTC-5′-Py (OP2) and 3′-CC ACC AAA GTA CCT ATG GTC-5′-Py-5′-CTG GTA TCC ATG AAA CCA CC-3′ (OPO2)

NHS-Py-NHS was dissolved in 500 μL acetonitrile and CPG-3′-CC ACC AAA GTA CCT ATG GTC-amine-5′ (1 μmole scale) was added to the solution and the mixture was shaken at r.t. for 12–18 h. The mixture was filtered and washed twice with 1 mL acetonitrile. The product (CPG-3′-CC ACC AAA GTA CCT ATG GTC-5′-Py-NHS) was added to a mixture of 300 μL 0.1 M sodium tetraborate–HCl buffer (pH 8.5), 56 μL DMSO and 120 μL purified 3′-CC ACC AAA GTA CCT ATG GTC-amine-5′ (30 O.D.)/H_2O followed by shaken slowly at r.t. for 12–18 h. After filtration, the product was washed twice with 1 mL acetonitrile and then deprotected with 1 mL ammonium hydroxide at 80 °C for 1 h. The product was purified with HPLC and the pure OP2 and OPO2 were obtained (the yield could not be calculated). MS [M^+]: (MALDI-ToF (linear mode)) calcd. for OP2, 6587.57; found, 6593.7 and calcd. for OPO2, 12810.7; found, 12848.8.

2.3. Hybridisation and fluorescence measurement

1 M SSPE buffer (pH 7.4, Sigma) was used as the standard hybridisation solution for this study. The SSPE solutions of 25 nM probes (each of OPO and OP) and various concentration of tODN were shaken at 25 °C for 3 h. Then the fluorescence spectra were measured on a RF-500 spectrofluorophotometer.

2.4. Agarose gel electrophoresis of the oligonucleotides

The oligonucleotide and 20 bp DNA ladder (TaKaRa, Japan) were electrophoresed on agarose gel in 0.5 × TAE buffer and then the electrophoresed gel was stained with ethidium bromide

and photographed under UV-irradiation with a digital camera (Model COOLPIX 4300, Nikon, Tokyo, Japan).

2.5. HR-TEM imaging

10 μL solutions of OPO hybrid (75 pmol of OPO1, 75 pmol of OPO2 and 150 pmol of tODN) and OP hybrid (75 pmol of OP1, 75 pmol of OP2 and 75 pmol of tODN) were dropped on copper grid, respectively, then the grids were freeze-dried. The powder on the grids was removed by blower and then the TEM images were obtained.

2.6. Melting experiments

The melting curve of each hybrid was obtained by determining the PL intensity at 420 nm (monomer emission) and 510 nm (excimer emission) of the solution as a function of temperature. It took about 20 min for the solution to reach temperature equilibrium after each 5 °C incremental increase. The solution in the cuvette was stirred with magnetic stirrer and the temperature was measured with a platinum resistance thermoprobe inserted into the heating block near to the cuvette. In our experiments, the relative PL intensity is corresponded to the level of PL intensity between the highest (100%) and the lowest (0%) PL intensity in 30–75 °C.

3. Results and discussion

Structure of our OPO probes and the hybrid of them with target ODNs are represented in Fig. 1. In OPO1 probe, bisfunctional pyrene derivative is linked to a 3′ ends of two identical ODNs, which have complementary sequences to the half of target ODN (tODN) on the direction from 3′ end to 5′ end. On the other hand the pyrene of OPO2 probe is linked to 5′ ends of two identical ODNs containing the complementary sequences to the other half of tODN on the direction from 5′ end to 3′ end. When the tODN is added to the probes (OPO1 and OPO2), the probes hybridize initially with the tODN to locate the pyrene derivatives in neighboring position enabling excimer emission much like the conventional OP probes (see Fig. 1(a)) [15–17]. However, subsequent structural evolution of our OPO probe is different from that of OP probe since our OPO probe has additional ODN sequence capable of further hybridisation with another tODN after initial hybridisation. When the further hybridisation is occurred between the hybrid of OPO1, OPO2 and tODN and a half (complementary to OPO1 or OPO2) of tODN, the other half of the tODN and probe are capable of selective hybridisation with each other or another probe (OPO1 or OPO2) and tODN out of the hybrid. In the case of the latter, it is possible that the hybrid will consecutive hybridize with another tODN and probes until the hybrid has reached limited compact structure. However, since a intra-structure hybridisation must have higher binding constant, the OPO probes and tODN are subjected to build up cruciform DNA hybrid, a core-shell (pyrene-ODN) nanodot structure in aqueous environment, with stable pyrene aggregate as a core unit by the former hybridisation process (Fig. 1(a) OPO hybrid).

We synthesized OPO1 and OPO2 as well as the conventional fluorescence probes OP1 and OP2 which lack the structural stability of the core-shell nanodot as the reference probes (see Fig. 1). Bisfunctional pyrene derivative (NHS-Py-NHS) was prepared by Sonogashira coupling, followed by conjugation with ODNs capable of hybridizing with tODN as described above.

First, we examined the capability of the building blocks OPO1, OPO2 and tODN to undergo self-assembly into the desired cruciform DNA hybrid. The oligonucleotides (OP1, OP2, OPO1, OPO2 and tODN) and 20bp DNA ladder were electrophoresed on 3% agarose gel in 0.5 × TAE buffer and stained with EtBr (Fig. 2(a)). It was clearly observed that the single stranded ODNs ran as a fragment with a similar electrophoretic mobility (lanes 2, 3 and 5) to the double stranded market gene of the same length of oligonucleotides. Conventional OP hybrid (hybrid of OP1, OP2 and tODN) ran as a fragment with similar mobility (lane 4) to the double stranded 40 bp marker gene as expected. On the other hand, the band of the OPO hybrid (hybrid of OPO1, OPO2 and tODN) became gradually shifted to the low mobility region with the progress of hybridisation and finally showed stronger fluorescence at the position with

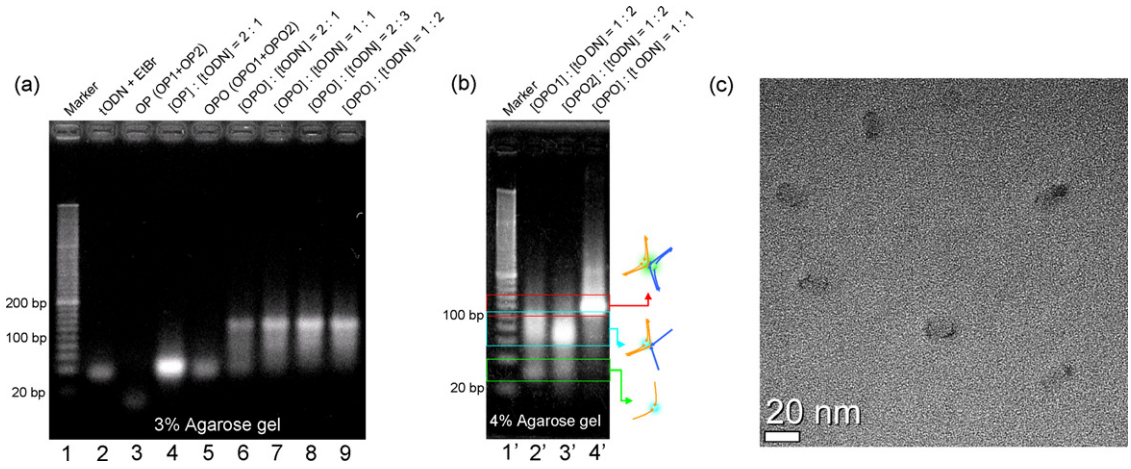

Fig. 2. Gel electrophoresis and TEM image: (a) 3% agarose gel of probes (OPO and OP) and tODN; (b) 4% agarose gel of OPO with tODN and schematic representations of corresponded hybrids to each bands; (c) HR-TEM image of the hybrids between OPO and tODN.

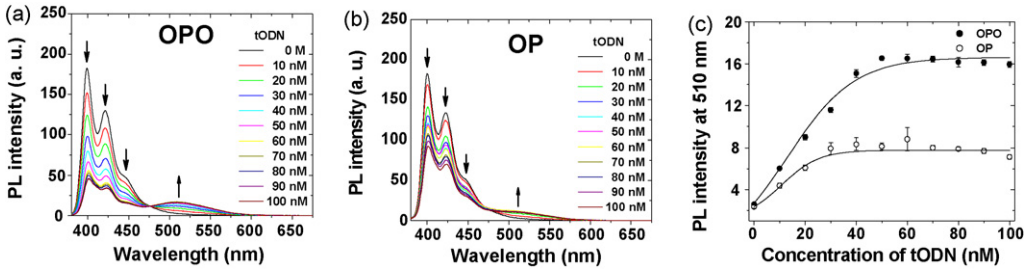

Fig. 3. Fluorescent spectra of (a) OPO probes (25 nM each of OPO1 and OPO2); (b) OP probes (25 nM each of OP1 and OP2) with increasing concenstration of tODN; (c) excimer emission profiles (average values of three times measurements) of OPO (25 nM each of OPO1 and OPO2) and OP (25 nM each of OP1 and OP2) probes depending on concentration of tODN.

corresponding mobility of ~120 bp marker gene (lanes 6–9). Moreover, it is difficult to find a trace of hybrids having less mobility than the strongly fluorescent bend. These results imply that the hybridisation between OPO1, OPO2 and tODN forms a dominant hybrid. To investigate the composition of the dominant hybrid, the OPO probes and tODN were electrophoresed in 4% agarose gel as well (Fig. 2(b)). The OPO hybrid ran as a fragment 100–120 bp of marker gene again in 4% agarose gel (lane 4′). Both of the hybrids of unpaired OPO1 and OPO2 with tODN mainly ran as a fragment of approximately 60–100 base pairs of marker gene and these results indicate that the probes easily hybridize with two tODN (see lanes 2′, 3′ and schematic representation of Fig. 2(b)). Since the hybrids of lanes 2′ and 3′ have lower mobility than their expected mobility and the mobility of hybrid of lane 4′ do not have a big difference from the mobility of lanes 2′ and 3′, we cannot expect that the dominant hybrid of lane 4′ is a more evolutionary structure than the cruciform hybrid. Archer and co-workers have reported a large star branched DNA have less mobility than linear one in gel electrophoresis [18]. According to the report, we can expect that the cruciform DNA hybrid have the lower mobility than the expected mobility corresponding to 80 bp of marker due to the shape effect. As a result, we can expect that the hybridisation between OPO1, OPO2 and tODN formed the cruciform DNA hybrid, composed of one of OPO1, one of OPO2 and two of tODN, as desired above. As shown in Fig. 2(c), the cruciform DNA hybrids were clearly shown monodispersed nanoparticles, but a discriminable image of the hybrid between OP1, OP2 and tODN was not obtained by HR-TEM.

Fig. 3(a)–(c) show the fluorescence sensing results for OPO (25 nM each of OPO1 and OPO2) and OP (25 nM each of OP1 and OP2) probes with various concentrations of the tODN in SSPE buffer (pH 7.4). On excitation at 365 nm, unhybridized probes (0 M of tODN) showed typical fluorescence of pyrene monomer emission (peaks at 400, 420 and 445 nm). As shown in Fig. 3(b) and (c), the excimer emission form the hybrids conventional OP probes is linearly increased in 0–30 nM of tODN at the expense of the decreased monomer emission. Beyond the tODN concentration of 40 nM, the excimer emission is virtually saturated with unexpectedly small decrease. These rather slow decreases of excimer emission of OP (also of OPO) in excess tODN implies that a strong tendency of probe components (OP1 and OP2) to hybridize to the same tODN [16]. Most importantly, the fluorescence modulation effect of OPO hybridisation is far larger than that of OP hybridisation as can be compared from Fig. 3 and Table 1. In case of OPO probes, it is also noteworthy that the excimer emission increased linearly in the 0–50 nM concentration of tODN and reached the higher saturation intensity than that of OP probes, even though they have the same number of pyrene moieties. These features, the higher excimer emission intensity at saturation and wider detection range, of OPO probes are likely due to the core-shell nanodot architecture, developed in aqueous environment, comprising OPO probes and tODN. The core of the OPO hybrid nanostructure in aqueous solution, containing two pyrene moieties in restricted space, gives a chance to form a pyrene excimer more efficiently compared to that in OP case. As shown in the electrophoresis experiment, OPO probes build the cruciform DNA hybrid from low concentration of tODN (lane 6). With increasing concentration of tODN, it is assumed that the number of hybrids, which efficiently generate excimer emission, increases until the tODN concentration reaches to the essential ratio of OPO and tODN to build the hybrid. Consequently, the detection range of OPO probes indicates that the essential ratio of OPO probes and tODN in the hybrid is 1:1 ([[OPO1] + [OPO2]]: [tODN]) and this ratio is consistent with the composition of hybrid determined by the electrophoresis measurements. These features of wider detection range and higher excimer emission intensity are very useful for the real-time PCR monitoring the process of nucleic acid amplification in real time by using fluorescence techniques [19].

Melting temperature (T_m) of DNA is important factor for determining stability of the DNA hybrid. Most of methods for measuring T_m value, depending on the absorbance at 260 nm, need high concentration (about 1 μM) of the sample. While fluorescence has a benefit for measuring T_m value with small amount of sample due to its higher sensitivity, it is difficult to apply a

Table 1
Quantum yields of OP and OPO hybrids

	QY[a]	$QY_{excimer}$[b]
OP hybrid	0.23	0.06
OPO hybrid	0.20	0.09

Fluorescence quantum yields (QY) were determined by using quinine sulfate in 1N H_2SO_4 as a standard (QY = 0.545).
[a] Over all quantum yield.
[b] Quantum yield of excimer emission.

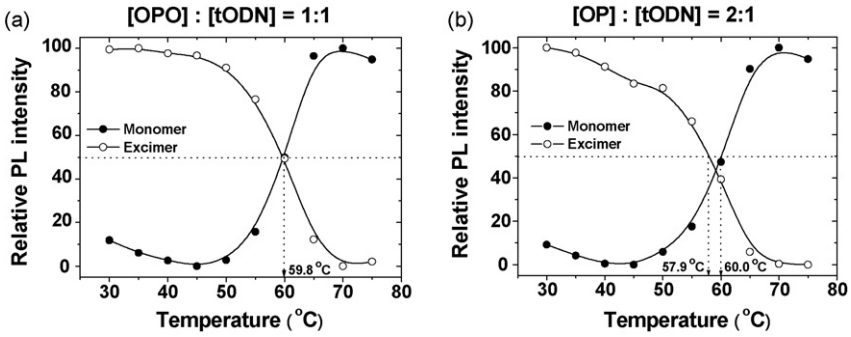

Fig. 4. Dissociation profiles of (a) the hybrid between OPO1, OPO2 and tODN and (b) the hybrid between OP1, OP2 and tODN, prepared by measuring excimer and monomer fluorescence intensities at 510 and 420 nm, respectively, as a function of temperature. The concentration of each probe was 25 nM.

fluorescent probe to the measurement of T_m, for the reason that its quantum efficiency is also sensitive to temperature change. In the case of conventional OP probe, while the T_m measured by monomer emission is close to the absorbance dependent T_m value, the T_m measured by excimer emission is slightly lower value due to the more temperature sensitive excimer emission [16]. As shown in Fig. 4(b), this report is consistent with our melting profiles of OP probe. However, the melting profiles of OPO hybrid is far from the OP hybrid. The decrease of excimer emission has lower slope than monomer emission in the section of 30–45 °C and the T_m by eximer emission is in good accord with the T_m by monomer emission (see Fig. 4). This feature, the high stability of excimer emission intensity as a function of temperature, of OPO hybrid is also likely due to the core-shell nanodot architecture comprising OPO probes and tODN. As a result, this feature produce the higher reliability in sensing experiment than OP probe (see Fig. 3(c)) and make us determine the T_m value by a single channel fluorescent measurement with small amount of sample for detection of genetic mutation.

4. Conclusion

We have designed and demonstrated a novel fluorescent probe working on the principle of fluorescence modulation with improved detection capability via building of DNA nanoarchitecture with target ODN. Since this novel OPO probe showed wide detection range, high-excimer emission efficiency and high reliability of excimer emission intensity, the probe is capable of application to diagnosis of genetic disease and detection of increased DNA copy number and occurrence of mutation in a real-time PCR.

Acknowledgments

This work was supported in parts by the Korea Science and Engineering Foundation (KOSEF) through the National Research Laboratory Program funded by the Ministry of Science and Technology (no. 2006-03246) and the Korea Health 21 R&D Project by Ministry of Health & Welfare of Korea (02-PJ1-PG1-CH08-0002).

References

[1] C.A. Stein, Y.-C. Cheng, Science 261 (1993) 1004.
[2] G.J. Hannon, Nature 418 (2002) 244.
[3] K.K. Mantripragada, P.G. Buckley, T.D. de Ståhi, J.P. Dumanski, Trends Genet. 20 (2004) 87.
[4] U. Feldkamp, C.M. Niemeyer, Angew. Chem. Int. Ed. 45 (2006) 1856.
[5] J.J. Storhoff, C.A. Mirkin, Chem. Rev. 99 (1999) 1849.
[6] Z. Junhui, C. Hong, Y. Ruifu, Biotechnol. Adv. 15 (1997) 43.
[7] W. Tan, K. Wang, T.J. Drake, Curr. Opin. Chem. Biol. 8 (2004) 547.
[8] N.L. Rosi, C.A. Mirkin, Chem. Rev. 105 (2005) 1547.
[9] J.J. Gooding, Electroanalysis 14 (2002) 1149.
[10] S.M. Waybright, C.P. Singleton, K. Wachter, C.J. Murphy, U.H.F. Bunz, J. Am. Chem. Soc. 123 (2001) 1828.
[11] E. Winfree, F. Liu, L.A. Wenzler, N.C. Seeman, Nature 394 (1998) 539.
[12] W.M. Shih, J.D. Quispe, G.F. Joyce, Nature 417 (2004) 618.
[13] A. Condon, Nat. Rev. Genet. 7 (2006) 565.
[14] C.K. Lim, J.S. Lee, T.H. Ha, I.C. Kwon, C.H. Ahn, S.Y. Park, J. Photochem. Photobiol. A 188 (2007) 149.
[15] P.L. Paris, J.M. Langenhan, E.T. Kool, Nucl. Acid Res. 26 (1998) 3789.
[16] M. Masuko, H. Ohtani, K. Ebata, A. Shimadzu, Nucl. Acid Res. 26 (1998) 5409.
[17] A.A. Martí, X. Li, S. Jockusch, Z. Li, B. Raveendra, S. Kalachikov, J.J. Russo, I. Morozova, S.V. Puthanveettil, J. Ju, N.J. Turro, Nucl. Acid Res. 34 (2006) 3161.
[18] S. Saha, D.M. Heuer, L.A. Archer, Electrophoresis 27 (2006) 3181.
[19] R.T. Ranasinghe, T. Brown, Chem. Commun. (2005) 5487.